Interface-Sensitive Micro-Imaging Based on X-Ray Reflectivity

It is important to understand interfaces since they are omnipresent in nature and control the properties of modern materials. Recently, the authors have succeeded in realizing X-ray reflectivity imaging of heterogeneous interfaces in ultrathin films. To visualize a wide viewing area, the image reconstruction scheme is employed instead of micro-beam scanning. The technique achieves image contrast by using the difference in reflectivity at each in-plane point in the thin film sample. X-ray reflectivity profiles at local positions on the sample can be obtained without using a micro beam, as equivalent information can be extracted from a series of wide X-ray reflection projection datasets collected as a function of grazing angle.

The authors have developed the X-ray reflectivity imaging technique [1-4]. A schematic of the experimental setup at BL-14B is shown in **Fig. 1**. In the experiment, the X-rays were monochromated to 16 keV by a double-crystal Si 111 monochromator having an energy resolution of 10^{-4}. The monochromatic X-rays were collimated to form a thin parallel beam. The primary collimating slit was set at 22.5 m from the wiggler source, to collimate the beam to 1 mm (horizontal, H) × 8 mm (vertical, V). The incident X-ray intensity was monitored throughout the experiment by an ionization chamber (D_0) set 0.45 m behind the primary slit. In front of the entrance window of D_0, a fixed width (100 mm, H) slit was attached to further cut the beam horizontally; thus, the final size of the incident beam was 0.10 mm (H) × 8 mm (V). The sample stage, which was set at 0.45 m downstream from D_0, is based on a high-precision goniometer with an accuracy of 0.001°. A rotational motor is vertically attached to an L-shaped stand fixed on the goniometer to realize in-plane rotation (φ-axis in **Fig. 1**). The samples were vertically mounted using a sample holder. The sample holder was equipped with two manual tilt stages. The parallel beam illuminated around 10 mm [H, the footprint length of the X-rays, is always long enough to cover the silicon substrate size (10 mm)] × 8 mm (V) of the sample surface at grazing-incidence geometry. The reflected X-rays were recorded by an X-ray CCD camera (pixel size 6.45 μm) set 0.30 m on the downstream side of the sample as a one-dimensional projection image, where the imaging conditions are in the near-field regime.

An X-ray reflectivity imaging example of buried heterogeneous interfaces is shown in **Fig. 2**. Here, a patterned ultrathin film was studied by the imaging approach. The sample was fabricated on a pre-cleaned silicon substrate by an Eiko DID-5A magnetron sputtering system. Under the top uniform Ti layer the heterogeneous layer consists of two groups of thin films, as shown in panel **a**: (i) Au thin films including the top-left polygon and bottom-right rectangle with different thicknesses; (ii) Ni thin films consisting of the bottom-left thick rectangle, top-right triangle and center-right thin bar with different thicknesses. Panel **b** is an X-ray reflectivity sinogram of the sample at a specific incidence angle corresponding to the wavevector transfer $Q_z = 4\pi \sin\theta/\lambda = 0.0502$ Å^{-1} (θ: the grazing incidence angle in **Fig. 1**, λ: X-ray wavelength), where obvious sinusoidal patterns are observed.

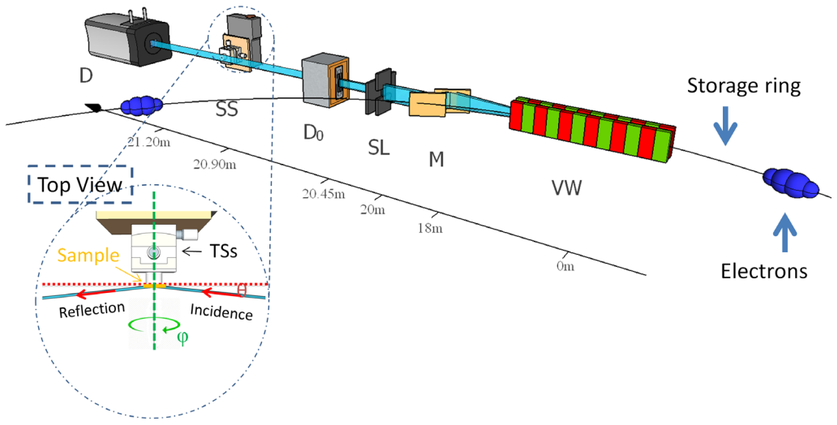

Figure 1: Schematic of the X-ray reflectivity imaging experimental set-up. VW: BL-14 vertical wiggler; M: monochromator; SL: 2D slit; D_0: ionization chamber, with a horizontal slit (0.05 mm, H); SS: sample stage on a goniometer; D: X-ray CCD camera. Inset is the enlarged image of SS from the top view: TSs: tilting stages. Reprinted, with permission, from reference [1].

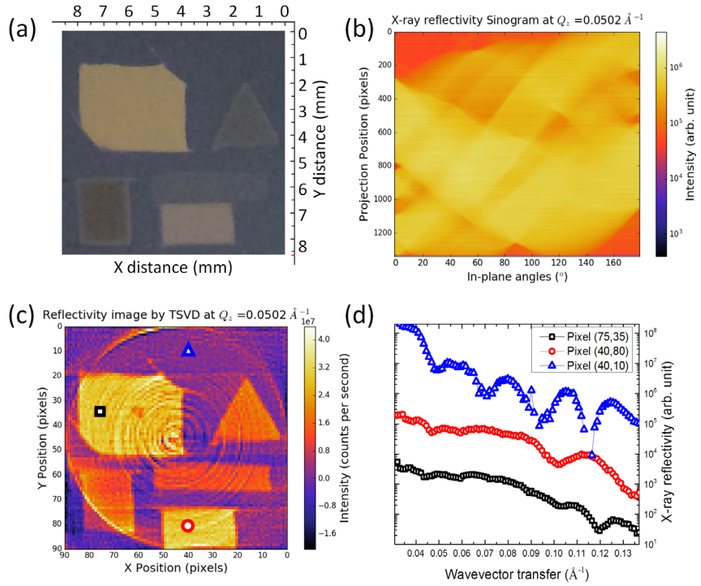

Figure 2: Typical X-ray reflectivity imaging data. **(a)** An optical image of a heterogeneous patterned (Au and Ni) ultrathin film sample before coating with a Ti uniform layer. **(b)** An X-ray reflectivity sinogram of the sample at Q_z = 0.0502 Å^{-1}. **(c)** A reconstructed X-ray reflectivity image of the sample at Q_z = 0.0502 Å^{-1}. **(d)** Three selected μXR profiles at local positions [as indicated by the same symbols in panel **(c)**] of the sample extracted from reconstructed X-ray reflectivity images. Reprinted, with permission, from reference [2].

The 1338 pixels are equally binned into 90 pixels (pixel length: 96 μm, 96 μm × 90 = 8.6 mm). The algebraic imaging reconstruction approach is employed to quantitatively reconstruct the X-ray reflectivity image. Panel **c** presents the corresponding reconstructed X-ray reflectivity image of the sample at Q_z = 0.0502 Å^{-1}. Although the sample is buried by the top Ti layer, the Au and Ni patterns are clearly observed by X-ray reflectivity imaging. At this wavevector transfer, the Au patterns produce higher reflectivity than the Ni patterns, thus giving a contrast between the patterns of the two different materials.

By scanning grazing angles, a series of X-ray reflectivity images sampled equally over a range of wavevector transfers is collected, thus μXR, which is the X-ray reflectivity profile at every micro-sized pixel, can be extracted. Panel **d** shows three selected μXR profiles. The pixel [40, 10] contains only a uniform Ti layer. The μXR profile confirms this point by displaying a sharp drop at Q_z = 0.042 Å^{-1} and equal-period interference fringes. At pixels [40, 80] and [75, 35], the μXR has an intensity drop around Q_z = 0.042 Å^{-1} and shallow oscillations below Q_z = 0.080 Å^{-1}. Beyond Q_z = 0.080 Å^{-1}, the μXR profile drops sharply and experiences deep oscillations. The two μXR profiles of Au patterns show different oscillation periods beyond Q_z = 0.080 Å^{-1}, indicating the different thicknesses of the patterns.

In the present research, X-ray reflectivity imaging was achieved by combining φ-scan and measurement of the 1D intensity profile of reflection projection. It has been demonstrated that the technique yields interface-sensitive images of ultrathin film samples. The new technique enables the non-destructive study of interfaces.

REFERENCES

[1] J. Jiang, K. Hirano and K. Sakurai, *J. Appl. Phys.* **120**, 115301 (2016).
[2] J. Jiang, K. Hirano and K. Sakurai, *J. Appl. Crystallogr.* **50**, 712 (2017) .
[3] K. Sakurai and J. Jiang, *J. Surf. Sci. Soc. Japan.* (2017) (in Japanese language, in press).
[4] J. Jiang and K. Sakurai, *Rev. Sci. Instrum.* **87**, 93709 (2016).

BEAMLINE

BL-14B

J. Jiang[1, 2], K. Hirano[3] and K. Sakurai[2, 1] ([1]Univ. of Tsukuba, [2]NIMS, [3]KEK-IMSS-PF)